Published in final edited form as:
Biochimie. 2011 July ; 93(7): 1139–1145. doi:10.1016/j.biochi.2011.03.011.

Characterization of the effect of TIMAP phosphorylation on its interaction with protein phosphatase 1

István Czikora[a,b], **Kyung-mi Kim**[c], **Anita Kása**[a], **Bálint Bécsi**[a], **Alexander D. Verin**[c], **Pál Gergely**[a,b], **Ferenc Erdődi**[a,b], and **Csilla Csortos**[a,*]

[a]Department of Medical Chemistry, University of Debrecen Medical and Health Science Center, Debrecen, Egyetem tér 1., H-4032, Hungary

[b]Cell Biology and Signaling Research Group of the Hungarian Academy of Sciences, Research Center for Molecular Medicine, University of Debrecen Medical and Health Science Center, Debrecen, Hungary

[c]Vascular Biology Center, Medical College of Georgia, CB-3210A, Augusta, GA 30912, USA

Abstract

TIMAP, TGF-β inhibited, membrane-associated protein, is highly abundant in endothelial cells (EC). We have shown earlier the involvement of TIMAP in PKA-mediated ERM (ezrin-radixin-moesin) dephosphorylation as part of EC barrier protection by TIMAP (Csortos et al., 2008). Emerging data demonstrate the regulatory role of TIMAP on protein phosphatase 1 (PP1) activity. We provide here evidence for specific interaction (K_a=1.80×10^6 M^{-1}) between non-phosphorylated TIMAP and the catalytic subunit of PP1 (PP1c) by surface plasmon resonance based binding studies. Thiophosphorylation of TIMAP by PKA, or sequential thiophosphorylation by PKA and GSK3β slightly modifies the association constant for the interaction of TIMAP with PP1c and decreases the rate of dissociation. However, dephosphorylation of phospho-moesin substrate by PP1cβ is inhibited to different extent in the presence of non- (~60% inhibition), mono- (~50% inhibition) or double-thiophosphorylated (<10% inhibition) form of TIMAP. Our data suggest that double-thiophosphorylation of TIMAP has minor effect on its binding ability to PP1c, but considerably attenuates its inhibitory effect on the activity of PP1c. PKA activation by forskolin treatment of EC prevented thrombin evoked barrier dysfunction and ERM phosphorylation at the cell membrane (Csortos et al., 2008). With the employment of specific GSK3β inhibitor it is shown here that PKA activation is followed by GSK3β activation in bovine pulmonary EC and both of these activations are required for the rescuing effect of forskolin in thrombin treated EC. Our results suggest that the forskolin induced PKA/ GSK3β activation protects the EC barrier via TIMAP-mediated decreasing of the ERM phosphorylation level.

Keywords

TIMAP; protein phosphatase 1; moesin; surface plasmon resonance

*Corresponding author. Department of Medical Chemistry University of Debrecen Medical and Health Science Center, Debrecen, Egyetem tér 1., H-4032, Hungary. Tel.: +36 52 412345; fax: +36 52 412566, csortos@med.unideb.hu (C. Csortos).

1. Introduction

TIMAP, TGF-β inhibited, membrane-associated protein, is considered as a member of the MYPT-family [1] of the regulatory subunits of protein phosphatase 1 (PP1). Specificity and localization of PP1 activity is ensured by the wide variety of its targeting/regulatory subunits, as PP1 is a holoenzyme consisting of the catalytic subunit (PP1c α, β (also called δ), γ1 or γ2 isoform), and one or two of its regulatory subunits [2]. TIMAP is the most abundant in endothelial cells (EC) [3] compared to other cell types. The vascular EC monolayer acts as a semiselective barrier between blood and the interstitium; and EC barrier integrity is critical to tissue and organ function. Phosphorylation level of many cytoskeleton and cytoskeleton-associated proteins plays crucial role in the EC barrier function [4–6]. In our previous work we measured transendothelial electrical resistance of control and TIMAP-depleted human pulmonary artery EC (HPAEC) monolayers and we have shown positive regulatory effect of TIMAP on pulmonary endothelial barrier function [7]. The absence of TIMAP enhanced the effect of barrier-compromising agents, thrombin and nocodazole; and attenuated the increase evoked by EC-protective agents, sphingosine-1-phosphate (S1P) and ATP.

Among the other MYPT-family members TIMAP shows the greatest similarity to MYPT3, as they share not only ankyrin repeats and the PP1c binding motif, typical for all members, but they equally have prenylation motif at their C-terminus as well [3, 5]. Both TIMAP and MYPT3 have specific phosphorylation sites and their phosphorylation seemed to influence their effect on the catalytic activity of PP1c [8, 9].

Interaction between TIMAP and PP1c has been suggested and has been shown recently by the employment of different model systems. Furthermore, possible substrates for TIMAP-regulated PP1 (LAMR1 and ERM proteins) were also identified [7, 8, 10, 11]. Here we report further evidences for protein-protein interaction between TIMAP and PP1c proteins; and details on the possible regulation of this interaction and PP1c activity by TIMAP phosphorylation.

2. Materials and Methods

2.1 Proteins and Reagents

Materials were obtained from the following sources: thrombin, GSK3β inhibitor (AR-A014418) Sigma (St Louis, MO); bacterial expression vector pGEX-4T-2 (4.9 kb) GE Healthcare (Piscataway, NJ); Protease Inhibitor Cocktail Set III EMD Biosciences (San Diego, CA); ROKα/ROCK-II, active enzyme Upstate (Lake Placid, NY); GSK3β New England (Ipswich, MA); forskolin and Protein Kinase A Calbiochem (Gibbstown, NJ); γ-^{32}P-ATP Izotóp Intézet Kft. (Budapest, HU). Antibodies: custom-made rabbit polyclonal anti-TIMAP antipeptide (NGDIRETRTDQENK) antibody: Zymed laboratories (San Francisco, CA), rabbit polyclonal anti-PP1cβ antibody: Upstate Biotechnology (Lake Placid, NY), rabbit polyclonal anti-PP1cα and anti-phosphoERM antibodies: Cell Signaling Technology, Inc. (Beverly, MA), mouse monoclonal antimoesin antibody: BD Biosciences Pharmingen (San Jose, CA); Alexa 488-, Alexa 594-conjugated secondary antibodies, Texas Red-phalloidin, and ProLong Gold Antifade medium: Molecular Probes (Eugene, OR). Substances for cell culturing were from Invitrogen Corporation (Carlsbad, CA). All other chemicals were obtained from Sigma (St Louis, MO).

2.2 Cell line, cell culture

Bovine pulmonary artery endothelial cells (BPAEC) (culture line-CCL 209) were obtained frozen at passage 8 (American Type Tissue Culture Collection, Rockville, MD), and were utilized at passages 17–22 as previously described [12]. Cells were maintained at 37°C in a

humidified atmosphere of 5% CO_2 and 95% air in MEM supplemented with 20% (v/v) fetal bovine serum (heat-inactivated), 1 % sodium pyruvate, 0.1mM MEM non-essential amino acids solution, 1 % antibiotic-antimycotic solution.

2.3 Immunofluorescence and immunoprecipitation

Immunofluorescence studies of BPAEC monolayers were performed as described in [7]. The cover slips were rinsed and mounted in ProLong Gold Antifade (Molecular Probes, Eugene, OR) and observed with a 60× objective on an Olympus Fluoview FV1000 microscope. Images were processed using PhotoShop Imaging software. Immunoprecipitation of PP1c from BPAEC was performed as described before [7].

2.4 Preparation of GST–moesin expression construct

Wild type moesin coding sequence was produced and sub-cloned into pGEX-4T-2 bacterial expression vector using standard molecular biological techniques. Namely, moesin coding sequence was amplified from HPAEC cDNA using forward primer: 5'-AAGAATTCCCATGCCCAAAACGATCAGT-3' and reverse primer: 5'-GGCTCGAGTTACATAGACTCAAATTCGTC -3'. The primers (Metabion International AG, Martinsried, Germany) contained appropriate restriction sites for subcloning. The DNA sequences of the constructs were confirmed by sequencing (Sequencing Facility, Biological Research Center of HAS, Szeged, Hungary).

2.5 Recombinant protein expression

E. coli BL-21 (DE3) (Bioline, Randolph, MA) transformed with pGEX-4T-2 containing glutathione S-transferase (GST) alone, or wild type cDNA of moesin fused with N-terminal GST, were induced with 0.1 mM isopropyl β-D-thiogalactoside and grown at RT with shaking for 3 hours. Cells were harvested by centrifugation and the fusion proteins were isolated from the sonicated lysates by affinity chromatography on glutathione Sepharose 4B (GE Healthcare, Piscataway, NJ) according to the manufacturer's protocol. Eluted GST fusion proteins were tested by SDS-PAGE and the identity of proteins were confirmed by Western blot. PP1cβ [13] and GST-tagged TIMAP and its mutant version [7] were produced as described before.

Glutathione S-transferase tag was removed by proteolytic cleavage with thrombin (Amersham Biosciences) according to the manufacturer's protocol. The GST-moesin fusion protein (corresponding to approximately 100 μg of total protein) coupled to glutathione Sepharose beads was incubated with 1 Unit of thrombin diluted in 1× PBS for 16 hours at RT. After that thrombin was removed from the eluted mixture by its binding to p-aminobenzamidine-agarose (Sigma) by rotation at RT for 30 minutes. The eluted thrombin cleaved protein was analyzed by SDS-PAGE.

2.6 Phosphorylation of TIMAP

Mono-phosphorylated TIMAP was prepared by thiophosphorylation of GST-TIMAP with PKA catalytic subunit (200 U of PKA/1 mg of TIMAP) in 50 mM Tris-HCl pH 7.5 containing 1 mM benzamidine, 1 mM PMSF, 2 mM DTT, 1 mM EGTA, 10 mM NaF, 200 mM $MgCl_2$, and 0.5 mM ATP-γ-S at 30°C for 60 min. Double-phosphorylated TIMAP was prepared by further thiophosphorylation of the mono-phosphorylated TIMAP with GSK3β (500 U of kinase/1 mg of TIMAP) in 20 mM Tris-HCl pH 7.5, 10 mM $MgCl_2$, 5 mM DTT containing 0.2 mM ATP-γ-S at 30°C for 30 min. Both thiophosphorylated TIMAP forms were extensively dialyzed in 50 mM Tris-HCl, pH 7.5 containing 0.1% 2-mercaptoethanol and 0.5% protease inhibitor cocktail to remove the excess of ATP-γ-S. In the SPR experiments and in the phosphatase assays we employed these thiophosphorylated GST-

TIMAP forms to avoid their possible dephosphorylation by PP1c. Using γ-^{32}P-ATP as phosphoryl donor substrate, the PKA or PKA/GSK3β induced extent of phosphorylation were estimated to be about 0.8 mol phosphate/mol TIMAP or 1.7 mol phosphate/mol TIMAP, respectively. To estimate the level of thiophosphorylation after the phosphorylation with ATP-γ-S we continued the incubation with freshly added ATP substrate and kinase. The phosphorylation level of GST-TIMAP with and without the extra additions and incubation time were compared by Western blot using phospho-serine specific antibody. We could not detect any further increase in the phosphorylation level of TIMAP after the addition of fresh kinase(s) and ATP. Therefore we assume that the extent of thiophosphorylations of TIMAP was similar to those values that were determined with the radioactive ATP substrate.

2.7 In Vitro Phoshatase Activity Assay

Phospho-moesin was prepared by phosphorylation of 0.5 mg/ml GST-cleaved recombinant moesin with 0.4 U/ml of Rho-kinase in Rho-kinase assay buffer (20mM MOPS pH 7.2, 25 mM glycerophosphate, 0.5 mM EGTA and 0.5 mM DTT) containing 1 μM microcystinLR, 5 mM $MgCl_2$, and 0.2 mM ATP at 30°C for 150 min. P-moesin was extensively dialyzed to remove microcystin and the excess of ATP. Recombinant PP1cβ (10 pmol) was assayed with 2 μM P-moesin for 30 min at 30°C in the presence or absence of 10 pmol wt, mutant or thiophosphorylated forms of GST-TIMAP. The reaction was started by the addition of the substrate, and stopped by the addition of hot 5X SDS loading buffer followed by immediate boiling of the samples for 10 min. Phosphorylation level of P-moesin before and after the phosphatase assay was determined by Western Blot using anti-phospho-ERM antibody. Densitometry of signals was performed using ImageJ 1.42q software (downloaded from: http://rsb.inf.nih.gov/ij). Phosphatase assays with MLC20 substrate were performed as described in [14]. Phosphatase activities were measured in four independent assays.

2.8 Surface Plasmon Resonance

Surface plasmon resonance experiments were performed on a Biacore 3000 instrument equipped with research grade CM5 sensor chips (Biacore AB, Uppsala, Sweden). CM5 surfaces were prepared at 25°C by the amine-cou plingmethod using reagents available from Biacore AB (N-ethyl-N'-Dimethylaminopropyl-carbodiimide [EDC] and N-hydroxysuccinimide [NHS], 1 M ethanolamine-HCl at pH 8.5). Flow cells were activated for 6 min with a solution containing 50 mM NHS and 200 mM EDC. Anti-GST antibody was diluted to 30 μg/ml in 10 mM Na-acetate (pH 5.0) and injected over the surface for 7 min at 10 μl/min flow rate. Excess reactive sites were subsequently blocked by injection of 1 mM ethanol-amine (pH 8.5). On the flow cell surfaces of the sensor chip either recombinant full length GST-TIMAP (wt), truncated (Δ1–71 aa) GST-TIMAP, and GST, or non-phosphorylated-, mono-, double-thiophosphorylated GST-TIMAP, and GST were coupled in 25 mM Tris-HCl (pH 7.4) containing 0.15 M NaCl, 1 mM DTT, 2mM $MnCl_2$ and 0.05% Surfactant P20 (running buffer). The amount of captured ligands was determined from the changes of the resonance signal expressed as response unit (RU). The amount of coupled wt and mutant GST-TIMAP was 1400–1500 RU. In experiments with the thiophosphorylated forms of TIMAP, the coupled amounts used were lower as follows: 420–550 RU for GST-TIMAP, 330–400 RU for GST-TIMAP-P, and 300–370 RU for GST-TIMAP-PP. To investigate TIMAP-PP1c association and dissociation, recombinant PP1cβ (analyte) was applied over the surfaces in concentrations of 0.2, 0.5, 1.0, 2.0 and 3.0 μM at a flow rate of 10 μl/min and the binding of PP1c was monitored as changes of the RU in time. The association phase of the interactions was monitored for 7 min and the dissociation phase in running buffer without the analyte was followed for 5 min. The control surface (e.g. GST) was treated identically to the ligand surfaces (e.g. GST-TIMAP forms) to determine unspecific binding, which was subtracted from the data obtained with the ligand surfaces.

Kinetic (association and dissociation rate constants: k_a and k_d) and equilibrium parameters (association constant: K_a) were derived from the sensograms using BIAevaluation 3.1 software with fitting the data to a simple 1:1 Langmuir interaction model.

2.9 Measurement of transendothelial electrical resistance

Transendothelial electrical resistance (TER) was measured dynamically across confluent monolayer in response to several treatments using an electrical cell-substrate impedance sensing system (ECIS, Applied Biophysics, Troy, NY) as described previously [15]. Decreases in monolayer resistance to electrical current flow, which correlated with paracellular gap formation were measured according to the method described by Giaever and Keese [16].

3. Results and Discussion

3.1 Effect of the phosphorylation level of TIMAP on its interaction with PP1cβ

Protein-protein interaction between wt as well as mutant GST-TIMAP and PP1cβ was studied by surface plasmon resonance (SPR) based binding technique on Biacore 3000 equipment. Immobilized GST-tagged truncated form of TIMAP, which does not contain the PP1c binding motif as the first 71 amino acids are deleted [7] or GST (data not shown), both employed as negative controls, failed to bind PP1c. However, specific interaction was detected between wt GST-TIMAP and PP1c as shown in Fig.1A. With the aid of the evaluation program of the BIACORE software, we estimated the association constant, $K_a=1.80\times10^6\ M^{-1}$, for the interaction of wt GST-TIMAP with PP1c using 1:1 binding models for the sensograms obtained with 0.2 μM, 0.5 μM, 1.0 μM, 2.0 μM, and 3.0 μM PP1c.

Phosphorylation of MYPT3, a member of the MYPT family with great similarity to TIMAP, by PKA was described recently [9]. In our previous work we utilized PKA activation in control and TIMAP depleted HPAEC to see whether TIMAP phosphorylation may influence ERM phosphorylation level and endothelial barrier function [7]. Parallel with our experiments, Li and coauthors [8] studied TIMAP phosphorylation in living cells and they identified two phosphorylation sites, namely Ser337 and −333 for PKA and for GSK3β, respectively. In the latter work, with the employment of phosphomimic recombinants of TIMAP, it was suggested, that the interaction of TIMAP with PP1c is influenced by the phosphorylation state of TIMAP. Therefore, we thiophosphorylated the recombinant wt GST-TIMAP with PKA or with PKA followed by GSK3β, to study the interaction of these thiophosphorylated forms of TIMAP with PP1c. The amounts of the immobilized ligands in this second set of experiments were about one third of the amount immobilized in the first set of measurements (representative sensograms shown in Fig.1B and 1A, respectively). The association constant ($K_a = 1.28\times10^6\ M^{-1}$) calculated for non-phosphorylated TIMAP-PP1c interaction in the second set of experiments was close to the value ($K_a = 1.80\times10^6\ M^{-1}$) determined with higher amount of the immobilized ligand. We found that PKA thiophosphorylation alone did not change the rate constant of complex formation (k_a), but decreased the rate constant of dissociation (k_d) for the mono-thiophosphorylated TIMAP-PP1c interaction compared to the corresponding values for non-phosphorylated TIMAP-PP1c. In case of PKA/GSK3β double-thiophosphorylated TIMAP both the k_a and the k_d were reduced. Accordingly, the association constants for TIMAP-PP1c ($K_a=1.28\times10^6\ M^{-1}$) and double-thiophosphorylated TIMAP-PP1c ($K_a=1.93\times10^6\ M^{-1}$) interactions are very similar, but for the mono-thiophosphorylated TIMAP-PP1c binding the $K_a=7.39\times10^6\ M^{-1}$ value is about four times larger suggesting a moderately stronger interaction (Fig1.B, Table 1).

The interaction between PP1cβ and TIMAP has been shown previously by IP and pull-down experiments [7, 8]. Our present results not only supported those data, but provided K_a values characteristic for the interaction. Our results clearly indicate that thiophosphorylation of TIMAP affects the kinetics, but does not or only moderately modifies the affinity of TIMAP-PP1c binding.

3.2 The effect of TIMAP phosphorylation level on PP1c activity

The ERM proteins are cytoskeleton/membrane binding proteins, their conformation and binding capacity affected by their phosphorylation state [17–19]. In our recent work it was shown that forskolin pretreatment rescued control cells from the effect of thrombin; however no rescuing was detected in TIMAP-depleted cells. We concluded that TIMAP might be involved in PKA-mediated ERM dephosphorylation as part of TIMAP-mediated EC barrier protection [7]. We speculated that PKA and/or PKA primed GSK3β phosphorylation of TIMAP may directly or indirectly affect ERM dephosphorylation. Therefore, next we studied the effect of TIMAP on phosphomoesin dephosphorylation by PP1c in *in vitro* phosphatase assays. As shown in Fig.2A and B, wt non-phosphorylated and mono-thiophosphorylated GST-TIMAP reduced considerably (~60% and ~50%, respectively) the PP1c activity toward this substrate, while the double-thiophosphorylated GST-TIMAP had negligible (<10%) effect. Control proteins, GST and mutant GST-TIMAP, did not influence significantly the PP1c activity. To clarify whether this effect of TIMAP is specific for the substrate, or for the phosphatase itself, we repeated the experiment with ^{32}P-MLC substrate and detected similar pattern of changes in PP1 activity (Fig.2C) indicating that the inhibitory effect of TIMAP is not substrate specific.

Yong et al. [9] reported that PKA phosphorylation of MYPT3 resulted in PP1c activation. They proposed that there is direct interaction between the N-terminal ankyrin repeat region and the phosphorylation site motif of MYPT3, and upon phosphorylation this interaction is significantly reduced. The results of our binding and activity assays also suggest that binding of non-phosphorylated TIMAP to PP1c may keep the phosphatase activity “silent” (at least toward the investigated substrates), but after double-phosphorylation of TIMAP, although the proteins remain bound, the phosphatase activity may “appear”.

Li at al. [8] also found increased PP1c activity in immunoprecipitates of phosphomimic TIMAPs compared to wt using small, artificial substrate for the PP1c assay. However, they did not report such inhibitory effect of the nonphosphorylated TIMAP what we detected with the phosphoprotein substrates. Less PP1c was immunoprecipitated with overexpressed phosphomimic TIMAP than that of wt and it was concluded that phosphomimic mutations decreased the association of TIMAP with PP1c. Our present results are in an apparent controversy with the above data, since we have not detected a decrease in the stability of the PP1c -TIMAP-thio-PP complex compared to PP1c-TIMAP as revealed by SPR-binding studies with recombinant proteins. With respect to binding kinetics, it remains to be elucidated if the slower association of TIMAP-thio-PP (k_a=1.01 × 10^3 $M^{-1}s^{-1}$) compared to TIMAP (k_a=4.68 × 10^3 $M^{-1}s^{-1}$) with PP1c may have an influence on the formation of immunoprecipitated complexes in cell lysates. We detected about the same amount of TIMAP protein in PP1c- immunoprecipitate after forskolin treatment of BPAEC which is believed to induce diphosphorylation of TIMAP with the involvement of PKA and GSK3β (see 3. 3) compared to the amount of TIMAP in PP1c-immunoprecipitate from control, untreated cells or from cells after thrombin challenge (Fig.3A). In addition, we did not observe significant change in the amount of PP1c in TIMAP-immunoprecipitates after the same set of treatments (Fig.3B). Based on the above data the controversies could not be simply resolved at this point. However, the possible differences in changes in the protein conformations by substituting phosphorylatable side chains with acidic (Asp, Glu) residues versus formation of “more physiological” phosphate/thiophosphate esters could be important

factors that may contribute to the variability of the results. It is possible, that upon the phosphorylation/thiophosphorylation of TIMAP we detected differences in its effect on PP1c activity because the conformation of the interacting protein surfaces changed due to the presence of the phosphate/thiophosphate group(s) on TIMAP. Even though, both the SPR-binding patterns with recombinant TIMAP and PP1c, and more importantly the IP results of native proteins clearly indicate that the TIMAP and PP1c proteins remain associated with each other.

3.3 Inhibition of GSK3β attenuates the effect of forskolin

Based on our previous results with control and TIMAP-depleted EC, we hypothesized that the rescuing effect of forskolin on the phosphorylation level of ERM proteins at the cell membrane in thrombin treated EC is in connection with the phosphorylation of TIMAP by PKA [7]. The *in vitro* phosphatase assays presented here indicate that the PKA and PKA/GSK3β phosphorylated mono- and double-thiophosphorylated forms of TIMAP affected the dephosphorylation of a phospho-moesin substrate differently. Therefore, to further test whether PKA activity alone, or PKA primed GSK3β phosphorylation of TIMAP as well is important in the regulation of ERM phosphorylation, we studied ERM phosphorylation level in BPAEC. Immunofluorescence experiments were performed without and with GSK3β inhibitor (AR-A014418) pretreatment of the cells followed by various additions (Fig.4A). GSK3β inhibition in control or forskolin treated cells caused slight increase in ERM phosphorylation at the cell boundaries compared to cells without addition of the GSK3β inhibitor (Fig.4A.a–b). After forskolin treatment the spikes at the cell boundaries disappeared on the majority of cells (Fig.4A.c), however the morphology of the GSK3β inhibited cells was more similar to that of control cells (Fig.4A.a and d) suggesting that PKA activation by forskolin may be followed by GSK3β activation too. Thrombin treatment of EC activates the Rho pathway resulting in ERM phosphorylation and activation [17, 19]. It was also shown that GSK3β becomes phosphorylated at the inhibitory Ser9 site after addition of thrombin [20, 21]. Accordingly, we detected ERM phosphorylation and barrier dysfunction (gap formation) after thrombin; and even more pronounced barrier dysfunction when the GSK3β activity was inhibited by the specific inhibitor, AR-A014418, in thrombin treated BPAEC (Fig.4A.e–f). More importantly, forskolin was not able to rescue the cells from the effect of thrombin when GSK3β activity was inhibited as gaps between the cells and spikes on the cell boundaries were still present (Fig.4A.h). In addition, we checked the P-ERM level in the cell lysates after the same treatments using Western blot (Fig.4B–C). With immunofluorescence, we detected the changes in P-ERM level mostly at the cell boundaries, but as we expected, with Western blot, which shows the total P-ERM level of the cells, the variance of signals was less apparent. On the other hand, our TER measurements supported the hypothesis that in the effect of forskolin both the activation of PKA and the activity of GSK3β are critical factors. The inhibition of GSK3β activity significantly attenuated the rescuing effect of forskolin in thrombin challenged cells (Fig. 4D). In agreement with the data of Li and co-workers [8] and our previous work [7] our new results indicate that both PKA and GSK3β activities play critical role in the determination of ERM phosphorylation level via phosphorylation of TIMAP.

3.4 Conclusions

Taken together, using surface plasmon resonance binding studies we showed specific protein-protein interaction between TIMAP and PP1c (K_a=1.80×10^6 M^{-1}). Mono-, or double-thiophosphorylation of TIMAP moderately modifies the strength of binding. Our findings by immunofluorescence and TER experiments, and *in vitro* phosphatase assays suggest that the forskolin evoked PKA/GSK3β activation decreases the ERM phosphorylation level at the cell membrane due to the double-phosphorylation of TIMAP and as a consequence relative activation of the PP1c in the PP1c-TIMAP complex.

Acknowledgments

This work was supported from the Hungarian Scientific Research Fund CNK80709 (GP), K68416 (EF), RO1-HL080675 (ADV), and R01-HL67307 (ADV), TÁMOP4.2.2.-08/1-2008-0019 DERMINOVA, TÁMOP4.2.1./B-09/1/KONV-2010-0007.

Abbreviations

BPAEC	bovine pulmonary artery endothelial cell
GSK	glycogen synthase kinase
EC	endothelial cell
ERM	ezrin-radixin-moesin proteins
HPAEC	human pulmonary artery endothelial cell
IP	immunoprecipitation
MLC20	20 kDa light chain of myosin
MYPT	myosin phosphatase targeting subunit
LAMR1	laminin receptor 1
PKA	protein kinase A
PP1	protein phosphatase 1
PP1c	catalytic subunit of protein phosphatase 1
RT	room temperature
S1P	sphingosine-1-phosphate
SPR	surface plasmon resonance
TER	transendothelial electrical resistance
wt	wild type

References

1. Ito M, Nakano T, Erdodi F, Hartshorne DJ. Myosin phosphatase: structure, regulation and function. Mol. Cell. Biochem. 2004; 259:197–209. [PubMed: 15124925]
2. Cohen PT. Protein phosphatase 1--targeted in many directions. J. Cell Sci. 2002; 115:241–256. [PubMed: 11839776]
3. Cao W, Mattagajasingh SN, Xu H, Kim K, Fierlbeck W, Deng J, Lowenstein CJ, Ballermann BJ. TIMAP, a novel CAAX box protein regulated by TGF-beta1 and expressed in endothelial cells. Am. J. Physiol. Cell Physiol. 2002; 283:C327–C337. [PubMed: 12055102]
4. Dudek SM, Garcia JG. Cytoskeletal regulation of pulmonary vascular permeability. J. Appl. Physiol. 2001; 91:1487–1500. [PubMed: 11568129]
5. Csortos C, Kolosova I, Verin AD. Regulation of vascular endothelial cell barrier function and cytoskeleton structure by protein phosphatases of the PPP family. Am. J. Physiol. Lung Cell. Mol. Physiol. 2007; 293:L843–L854. [PubMed: 17693486]
6. Mehta D, Malik AB. Signaling mechanisms regulating endothelial permeability. Physiol. Rev. 2006; 86:279–367. [PubMed: 16371600]
7. Csortos C, Czikora I, Bogatcheva NV, Adyshev DM, Poirier C, Olah G, Verin AD. TIMAP is a positive regulator of pulmonary endothelial barrier function. Am. J. Physiol. Lung Cell. Mol. Physiol. 2008; 295:L440–L450. [PubMed: 18586956]

8. Li L, Kozlowski K, Wegner B, Rashid T, Yeung T, Holmes C, Ballermann BJ. Phosphorylation of TIMAP by glycogen synthase kinase-3beta activates its associated protein phosphatase 1. J. Biol. Chem. 2007; 282:25960–25969. [PubMed: 17609201]
9. Yong J, Tan I, Lim L, Leung T. Phosphorylation of myosin phosphatase targeting subunit 3 (MYPT3) and regulation of protein phosphatase 1 by protein kinase A. J. Biol. Chem. 2006; 281:31202–31211. [PubMed: 16920702]
10. Adyshev DM, Kolosova IA, Verin AD. Potential protein partners for the human TIMAP revealed by bacterial two-hybrid screening. Mol. Biol. Rep. 2006; 33:83–89. [PubMed: 16817016]
11. Kim K, Li L, Kozlowski K, Suh HS, Cao W, Ballermann BJ. The protein phosphatase-1 targeting subunit TIMAP regulates LAMR1 phosphorylation. Biochem. Biophys. Res. Commun. 2005; 338:1327–1334. [PubMed: 16263087]
12. Tar K, Birukova AA, Csortos C, Bako E, Garcia JG, Verin AD. Phosphatase 2A is involved in endothelial cell microtubule remodeling and barrier regulation. J. Cell. Biochem. 2004; 92:534–546. [PubMed: 15156565]
13. Toth A, Kiss E, Herberg FW, Gergely P, Hartshorne DJ, Erdodi F. Study of the subunit interactions in myosin phosphatase by surface plasmon resonance. Eur. J. Biochem. 2000; 267:1687–1697. [PubMed: 10712600]
14. Erdodi F, Toth B, Hirano K, Hirano M, Hartshorne DJ, Gergely P. Endothall thioanhydride inhibits protein phosphatases-1 and-2A in vivo. Am. J. Physiol. 1995; 269:C1176–C1184. [PubMed: 7491907]
15. Schaphorst KL, Pavalko FM, Patterson CE, Garcia JG. Thrombin-mediated focal adhesion plaque reorganization in endothelium: role of protein phosphorylation. Am. J. Respir. Cell Mol. Biol. 1997; 17:443–455. [PubMed: 9376119]
16. Giaever I, Keese CR. A morphological biosensor for mammalian cells. Nature. 1993; 366:591–592. [PubMed: 8255299]
17. Mangeat P, Roy C, Martin M. ERM proteins in cell adhesion and membrane dynamics. Trends Cell Biol. 1999; 9:187–192. [PubMed: 10322453]
18. Matsui T, Maeda M, Doi Y, Yonemura S, Amano M, Kaibuchi K, Tsukita S, Tsukita S. Rho-kinase phosphorylates COOH-terminal threonines of ezrin/radixin/moesin (ERM) proteins and regulates their head-to-tail association. J. Cell. Biol. 1998; 140:647–657. [PubMed: 9456324]
19. Tsukita S, Yonemura S. Cortical actin organization: lessons from ERM (ezrin/radixin/moesin) proteins. J. Biol. Chem. 1999; 274:34507–34510. [PubMed: 10574907]
20. Eto M, Kouroedov A, Cosentino F, Luscher TF. Glycogen synthase kinase-3 mediates endothelial cell activation by tumor necrosis factor-alpha. Circulation. 2005; 112:1316–1322. [PubMed: 16129813]
21. Beckers CM, Garcia-Vallejo JJ, van Hinsbergh VW, van Nieuw Amerongen GP. Nuclear targeting of beta-catenin and p120ctn during thrombin-induced endothelial barrier dysfunction. Cardiovasc. Res. 2008; 79:679–688. [PubMed: 18490349]

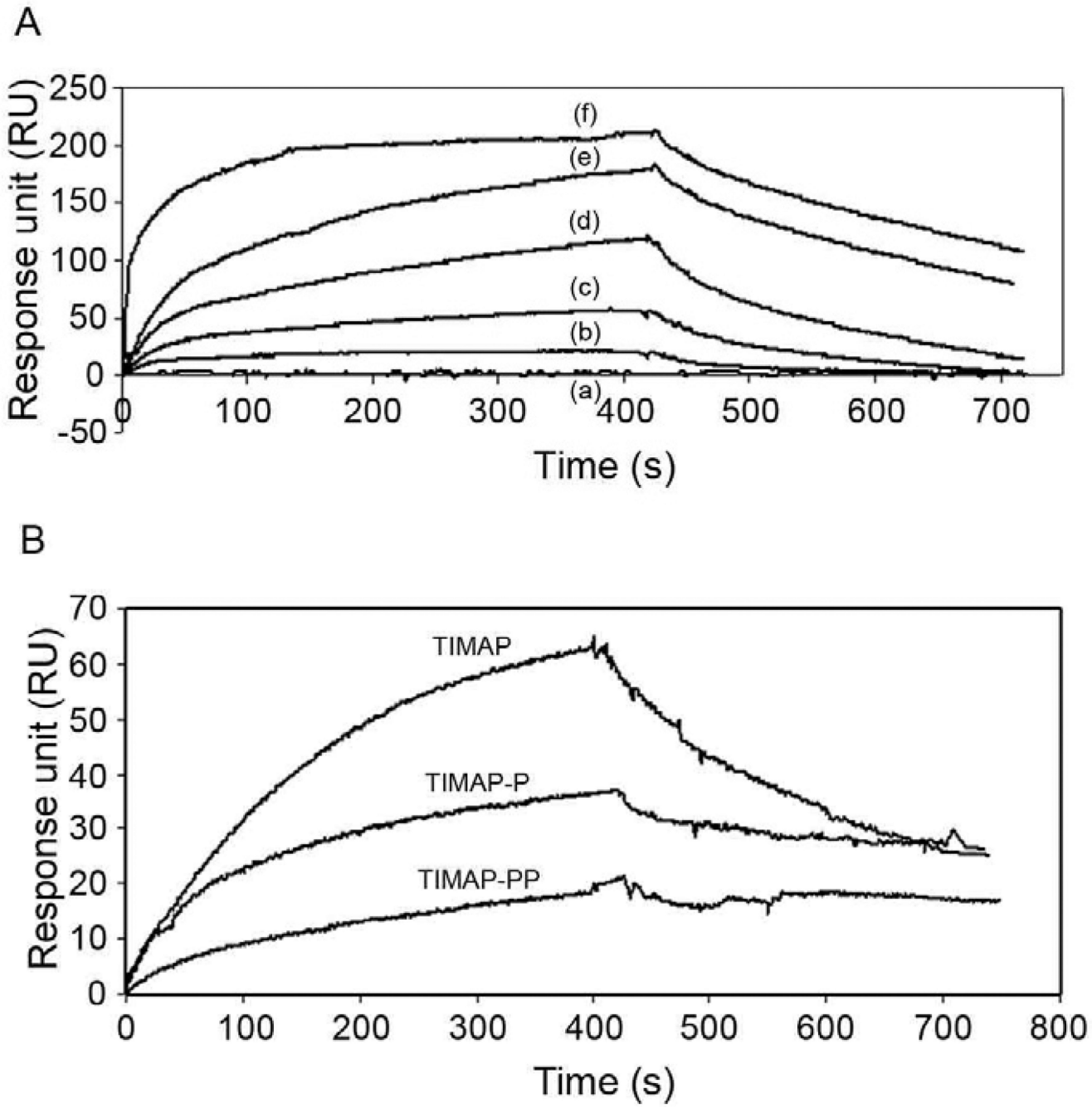

Fig. 1.

Interaction of non-phosphorylated and phosphorylated TIMAP forms with PP1c as revealed by surface plasmon resonance binding studies. Sensograms were obtained using Biacore 3000 instrument as described in Materials and Methods. (A) wild type (b–f) and mutant (a) GST-tagged TIMAP (1400–1500 RU) were immobilized on CM5 sensor chips coupled with anti-GST, and PP1c was injected over the surfaces at 0.2 μM (b), 0.5 μM (c), 1.0 μM (d), 2.0 μM (e), or 3.0 μM (a, f) concentrations. (B) Non-phosphorylated (542 RU), mono- (394 RU) and double-thiophosphorylated (369 RU) wt GST-TIMAP were immobilized on CM5 sensor chips coupled with anti-GST, and PP1c was injected over the surfaces at 3.0 μM

concentration. Shown are representative data of measurements performed at 3 or more different concentrations and each set was repeated once.

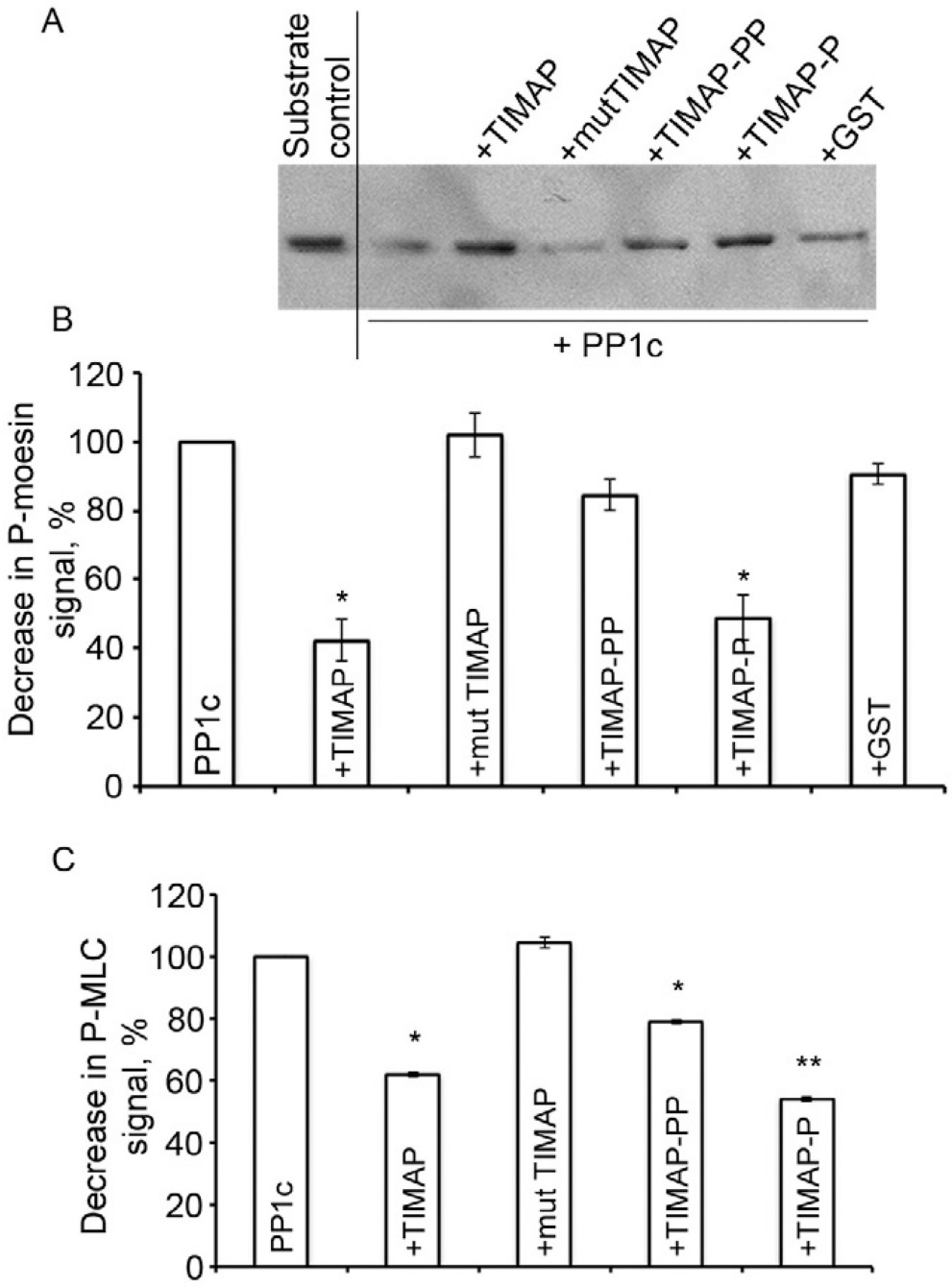

Fig. 2.

TIMAP phosphorylation state affects phosho-moesin and phospho-MLC20 dephosphorylation. Phospho-moesin (P-moesin) (A–B) and ^{32}P-labeled-phospho-MLC20 (P-MLC) (C) were used as substrate for dephosphorylation by PP1c in the absence or presence of wt GST-TIMAP, GST-TIMAP-thio-P, GST-TIMAP-thio-PP, mutant GST-TIMAP, or GST as described in Materials and Methods. (A) A representative Western blot with an anti-phospho-ERM antibody is shown to illustrate the effect of different additions on P-moesin phosphorylation level after 30 minutes of dephosphorylation. Substrate control on the left shows the phospho-moesin signal without phosphatase treatment. The decrease in the phospho signals of the phospho-moesin (B) or the phospho-MLC (C) after

dephosphorylation was expressed as percentage of the decrease detected in the phosphatase assay without any addition (100%). The amount of phosphatase present in the control phospho-MLC assay resulted in the release of $^{32}P_i$ which corresponded to about 20–25% of the total radioactivity of 2 μM MLC20 and this was taken as 100%. The results are presented as means ±SE from 4 independent experiments. Statistical analysis was done with Student's *t*-test. Significant changes are indicated by * ($P<0.05$) or ** ($P<0.01$) as a decrease in the phosphatase activity as compared to the enzyme activity detected in the phosphatase assay without any addition.

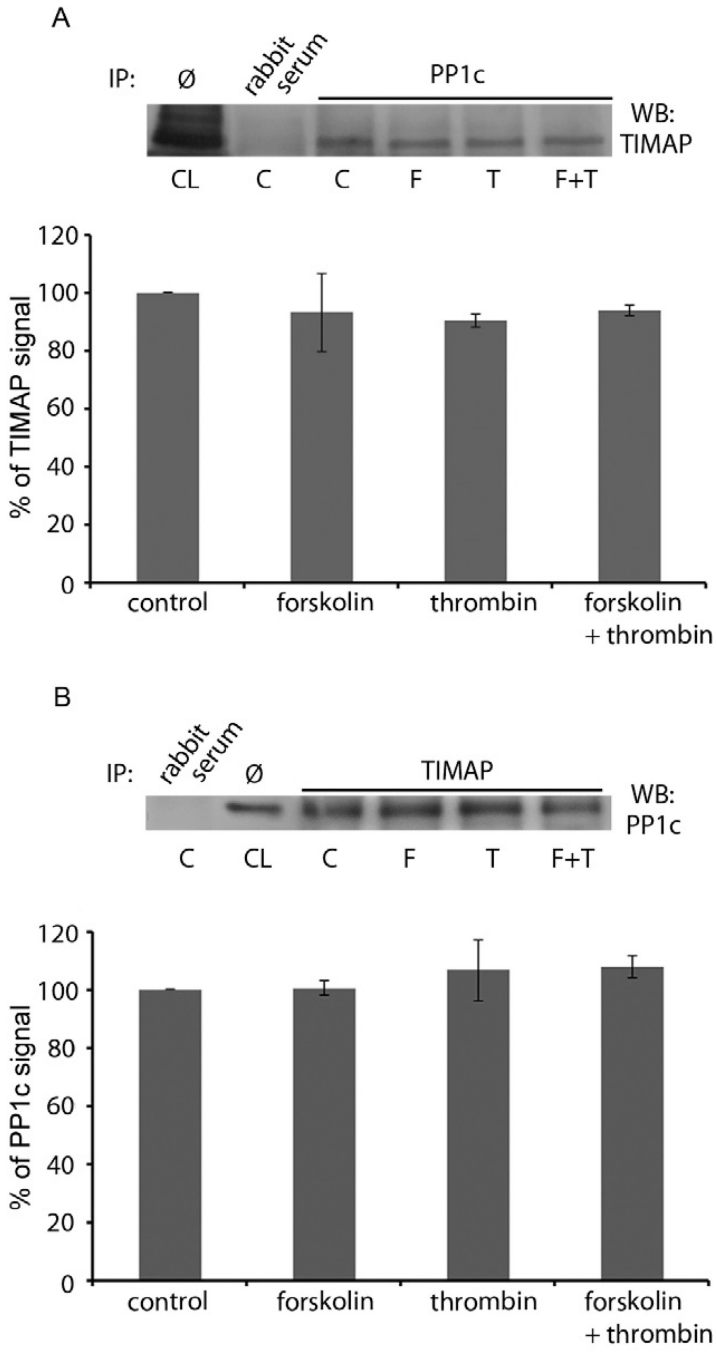

Fig. 3.

Phosphorylation level of TIMAP does not affect its binding to PP1c. PP1c (A) or TIMAP (B) was immunoprecipitated from lysates of untreated (control), forskolin (50μM, 10 min), thrombin (20 nM, 30 min), or forskolin (50μM, 10 min) followed by thrombin (20 nM, 30 min) treated BPAEC as described in Materials and Methods. The amounts are expressed as percentage of the TIMAP (A) or PP1c (B) signal obtained in the untreated control from three independent experiments. Statistical analysis (Student's t test) of the data did not show significant alterations ($P>0.05$). Above each graph representative Western blots of these experiments are shown. CL: cell lysate (Ø without immunoprecipitation), C: untreated

control, F: forskolin treatment, T: thrombin treatment, F+T: forskolin and thrombin treatment.

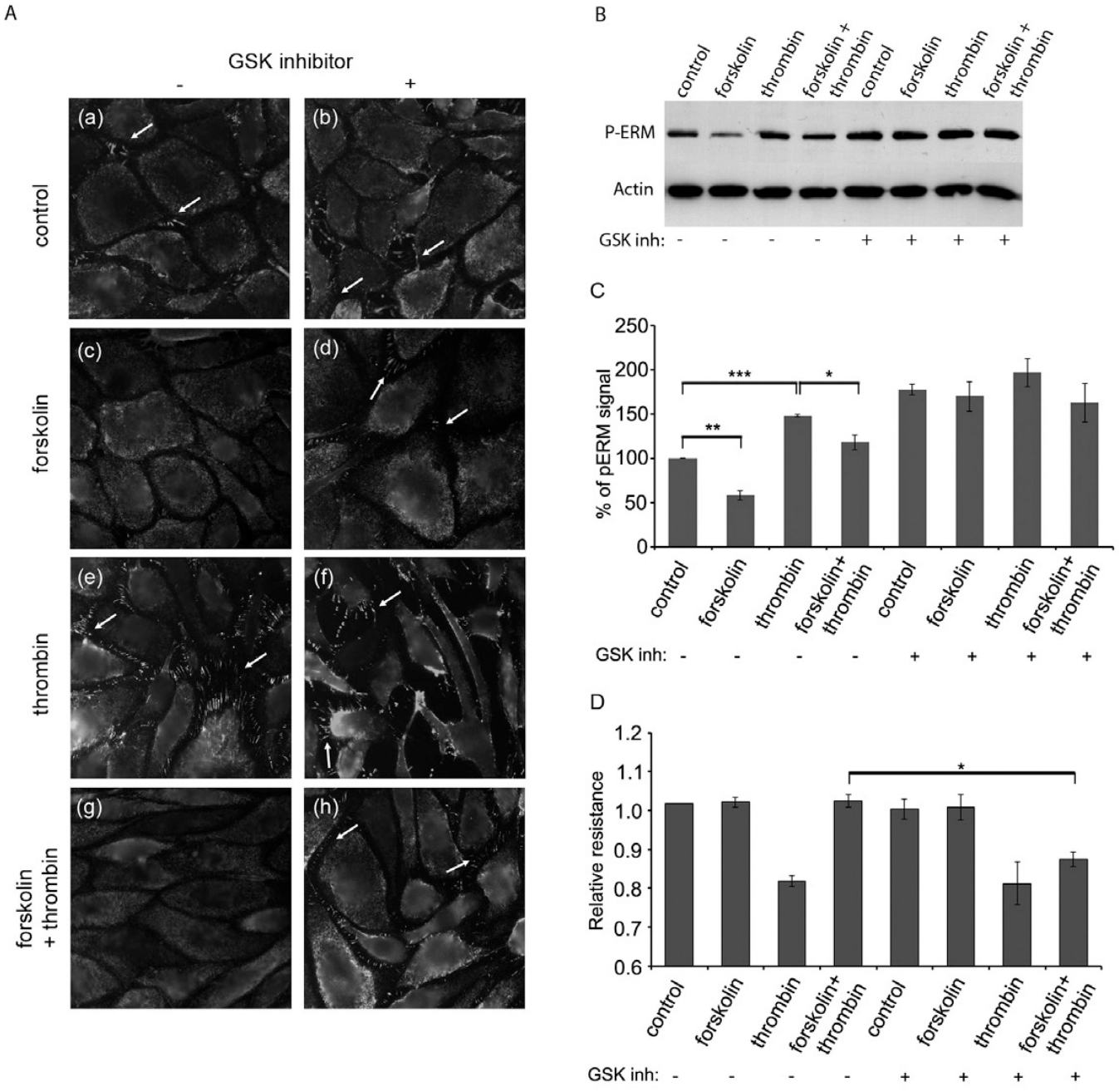

Fig. 4.

GSK3β inhibitor attenuates the effect of forskolin. (A) Control (a,c,e,g) and AR-A014418 pretreated (b,d,f,h) BPAEC monolayers were stained with anti-phospho-ERM primary antibody without (a–b) or with further various treatments as follows: 50μM forskolin (c–d) for 10 min; 20 nM thrombin (e–f) for 30 min; or 50μM forskolin for 10 min followed by 20 nM thrombin for 30 min (g–h). White arrows highlight spikes at the cell boundaries. (B) Detection of P-ERM by Western blot in BPAEC lysates after the same treatments as listed in part (A) of this figure. Actin was also detected in the samples as control. Shown are representative data of at least 3 independent experiments. Quantitative analysis of P-ERM signals are also shown (C). The results are presented as means ±SE from 3 independent experiments. The amounts are expressed as percentage of the P-ERM signal obtained in the

untreated cell lysates. (D) Measurements of transendothelial electrical resistance. After basal TER monitoring, BPAEC monolayers were pretreated with 20μM AR-A014418 or vehicle for 4 hours. After that 50μM forskolin or vehicle was added. When the TER values returned to similar values as controls (about 2 hours), the cells were treated with 20 nM thrombin. Initial resistance values varied between 750 and 850 Ω. Relative resistances detected at the time of maximal TER decline of the thrombin challenged cells are shown for each sample. Data are expressed as the average of at least three experiments ± SE.
Statistical analysis was done with Student's *t*-test. Significant changes are indicated by asterisks; * ($P<0.05$), ** ($P<0.01$), or *** ($P<0.001$).

Table 1

Kinetic and equilibrium parameters of the interaction of PP1c with different forms of GST-TIMAP. Non-phosphorylated, mono- and double-thiophosphorylated GST-TIMAP (wt) were immobilized on CM5 sensor chips coupled with anti-GST and PP1c was injected at 1.0, 2.0, and 3.0 μM concentrations. The parameters were derived from the sensograms as described in Materials and Methods. The rate constants of complex formation (k_a) and dissociation (k_d) shown in the table were obtained from the appropriate sensograms and expressed as mean ± SD from the three independent experimental settings, which were repeated at least once.

Ligand	Rate constant of complex formation, k_a (1/Ms)	Rate constant of dissociation, k_d (1/s)	Association constant, $K_a = k_a/k_d$ (1/M)
GST-TIMAP	$4.68(\pm1.32) \times 10^3$	$3.66(\pm0.88) \times 10^{-3}$	1.28×10^6
GST-TIMAP-P	$4.11(\pm0,37) \times 10^3$	$5.56(\pm1.12) \times 10^{-4}$	7.39×10^6
GST-TIMAP-PP	$1.01(\pm0.47) \times 10^3$	$5.22(\pm0.57) \times 10^{-4}$	1.93×10^6